Electronic Supporting Information (ESI)

Continuous 3D Printing Quantum Dots-Based Electrodes for Lithium Storage with Ultrahigh Capacities

Chao Zhang[†], *Kai Shen*[†], *Bin Li, Songmei Li and Shubin Yang**

Key Laboratory of Aerospace Advanced Materials and Performance of Ministry of Education, School of Materials Science and Engineering, Beihang University, 100191, Beijing, China

E-mail: yangshubin@buaa.edu.cn

[†] These authors contributed equally to this work.

Characterizations

Ink rheology: Rheological properties of the ink were measured by using a stress controlled DHR-2 rheometer (TA Instruments) with a 20 mm steel flat plate geometry. The apparent viscosity of ink was carried out at an angular frequency from 10^{-1} to 10^{2} s^{-1}. The storage (G') and loss (G'') moduli of inks as a function of shear stress from 10^{-1} to ~10^{3} Pa were obtain at a constant frequency of 1 Hz. Oscillatory time sweep with a constant shear rate of 1 Hz for 3 h was also carried out to demonstrate the structural stability of SnO_2 QDs/GO ink.

3D printing: First, as-prepared ink was loaded into a 3 mL syringes and extruded through a needle with a diameter of 200 μm by air pressure, provided by an air-powered fluid dispenser (DSP501N, Fisnar). The SnO_2 quantum dots/graphene (3DP-SnO_2 QDs/G) architectures were printed onto a substrate controlled by a benchtop robot (Fisnar F4200n) with a pre-editing program of micro-lattices, which were designed with a center-to-center rods spacing (L) of 800 μm and a rod diameter (d) of 200 μm. The optimal extrusion pressure and move speed of nozzle were 60 psi and 8 mm s^{-1}. Subsequently, the printed architectures were freeze-dried to remove the solvent and solidify the structure. Finally, a gas-based hydrazine hydrate reduction was implemented to reduce the GO.

Supplementary Figures

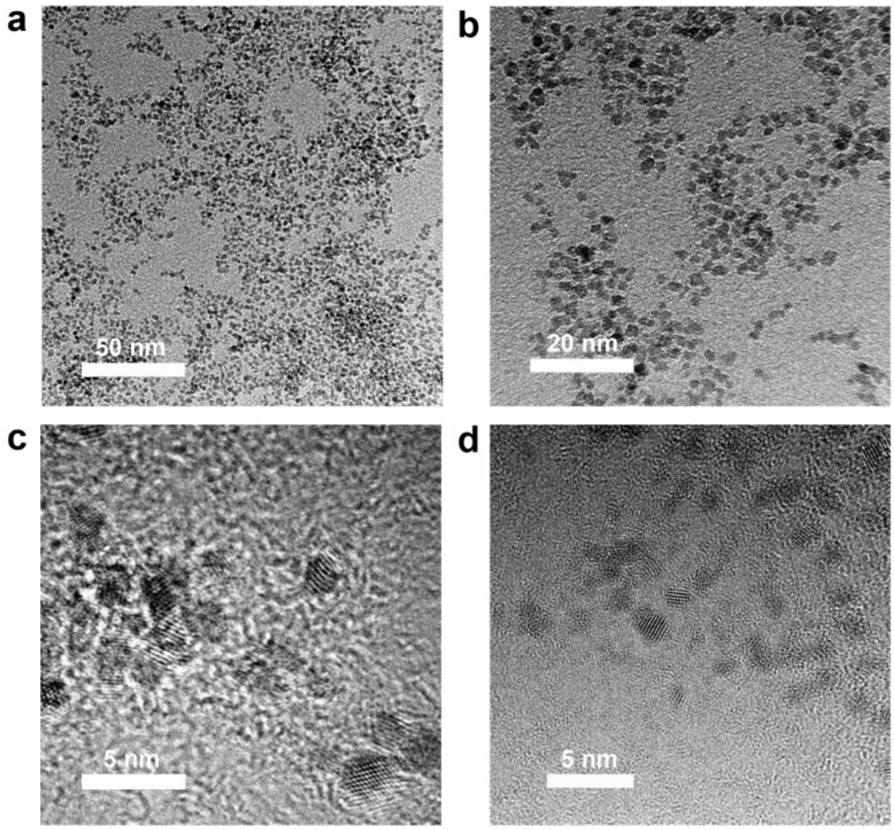

Fig. S1. TEM and HRTEM images of the SnO_2 QDs.

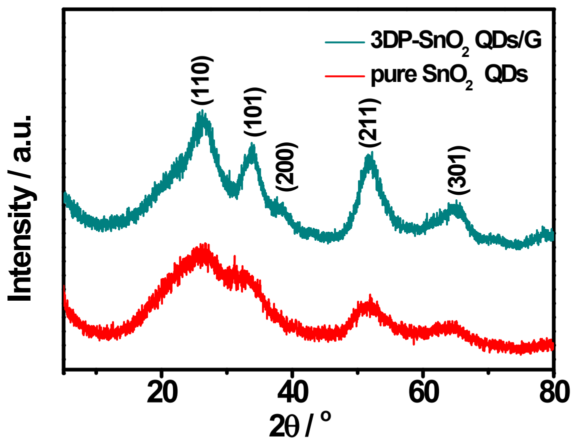

Fig. S2. XRD patterns of 3DP-SnO_2 QDs/G and pure SnO_2 QDs. The pure SnO_2 QDs and 3DP-SnO_2 QDs/G shows the same characteristic peaks, which are indexed as tetragonal rutile-like SnO_2, confirming the presence of SnO_2 in our printed architectures.

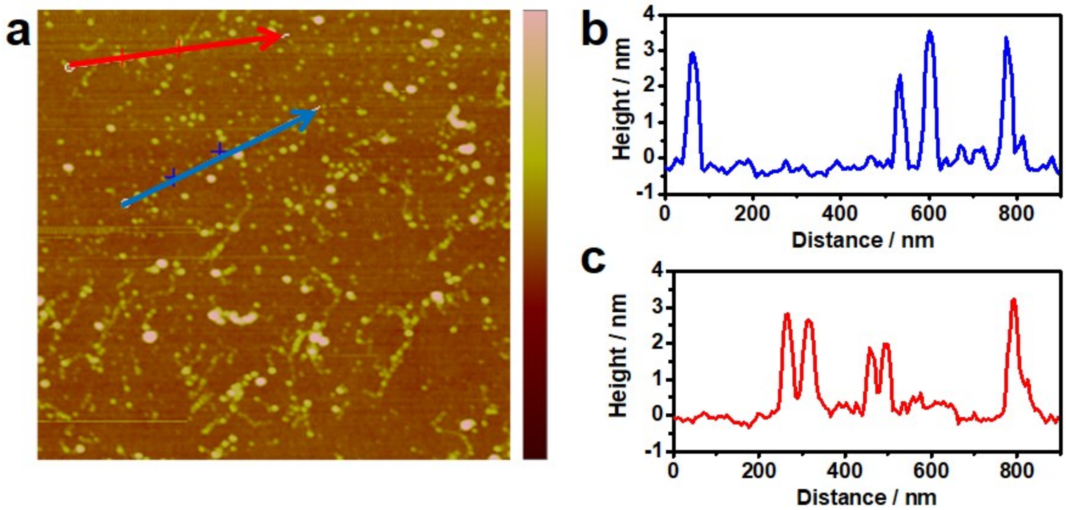

Fig. S3. a) AFM image of the SnO_2 QDs. b,c) Height analysis of the SnO_2 QDs along the blue and red line in a).

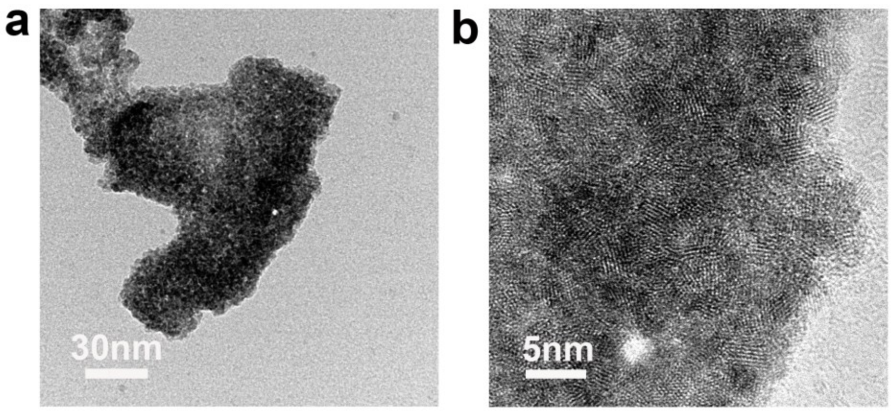

Fig. S4. a) TEM and b) HRTEM images of SnO_2 QDs obtained in the absence of NH_4Cl.

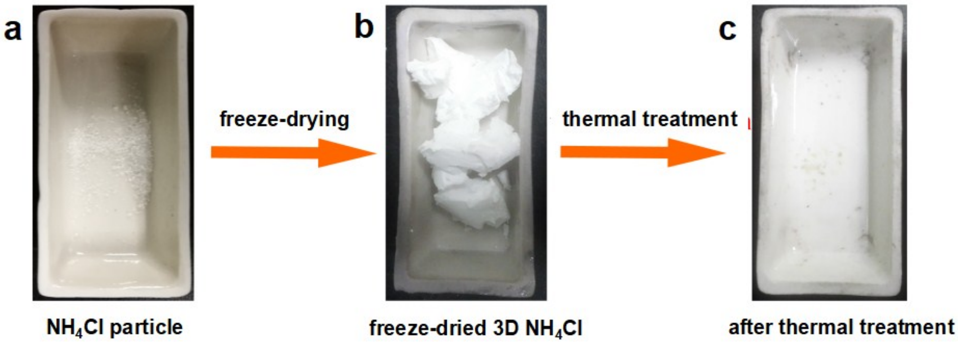

Fig. S5. Digital images of the controllable sol-gel approach in the absence of $SnCl_4$. Only three-dimensional NH_4Cl framework obtained after the freeze-drying process, and it decomposed after heat treatment.

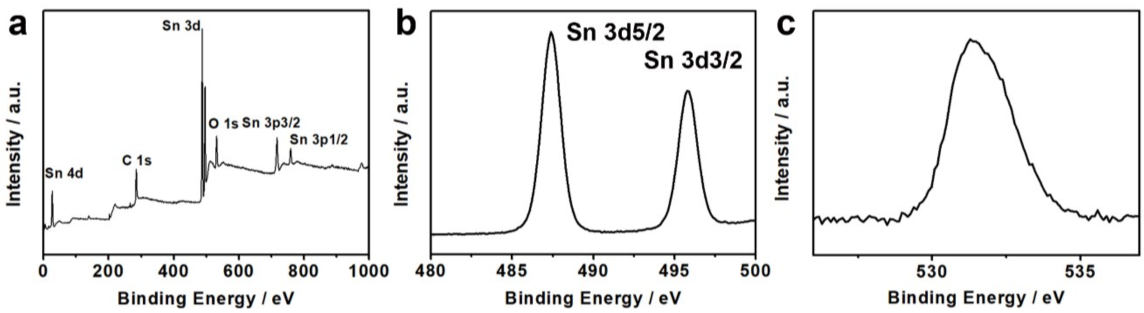

Fig. S6. a) XPS and b) high resolution Sn 3d and O 1s spectra of SnO_2 QDs.

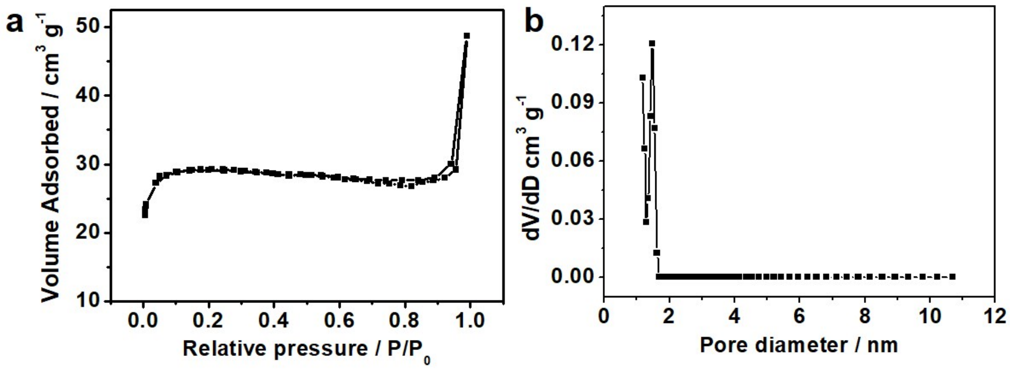

Fig. S7. a) The nitrogen adsorption-desorption isotherm and b) pore size distribution of SnO_2 QDs.

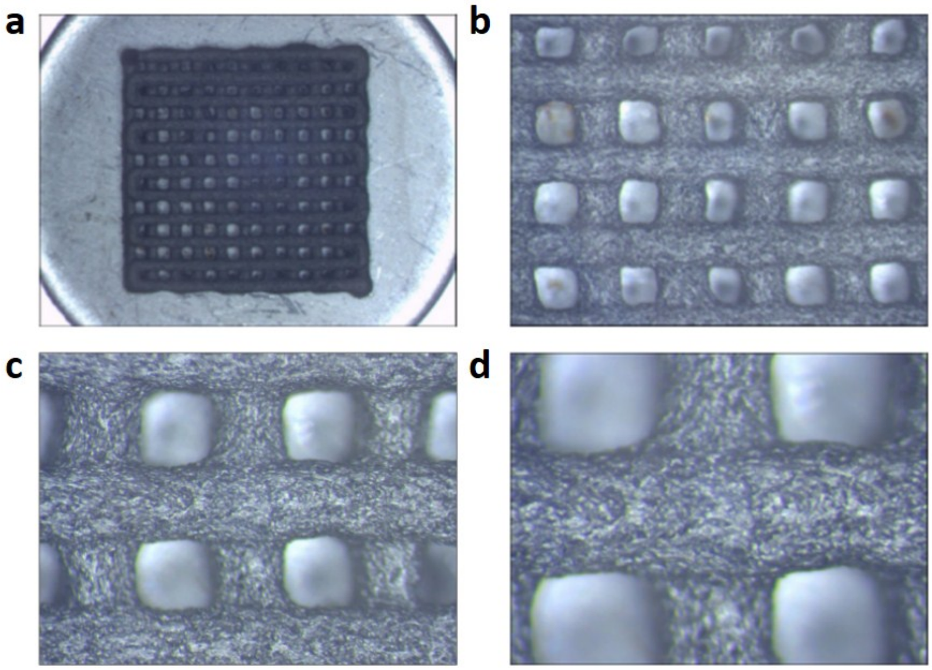

Fig. S8. Photos of 3DP-SnO_2 QDs/G architectures.

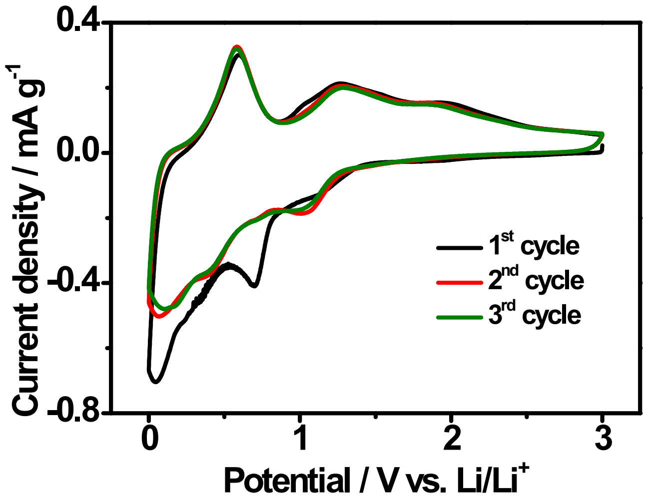

Fig. S9. Typical CV curves of 3DP-SnO_2 QDs/G architectures at a scan rate of 0.1 mV s^{-1}. Two pairs of dominant redox peaks at 0.03 and 0.58 V, 1.05 V and 1.3 V are attributed to the alloy and dealloy of Sn metal and transformation between SnO_2 and Sn, respectively.

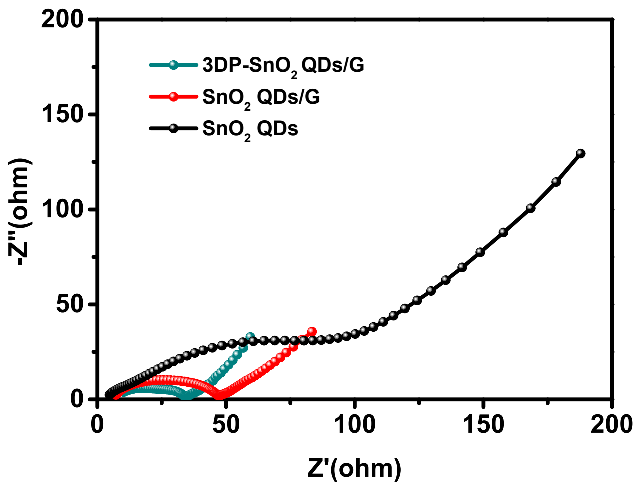

Fig. S10. Electrochemical impedance spectra (EIS) of 3DP-SnO_2 QDs/G, SnO_2 QDs/G and SnO_2 QDs.

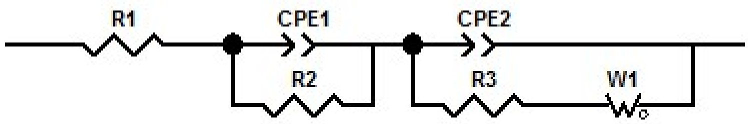

Fig. S11. The equivalent circuit diagram used for fitting the EIS profiles of 3DP-SnO_2 QDs/G, SnO_2 QDs/G and SnO_2 QDs. (R_1: the resistance of electrolyte; R_2: the resistance of the surface film formed on the electrodes; R_3: the charge-transfer resistance; CPE_1, CPE_1: constant phase element; W_1 : Warburg element)

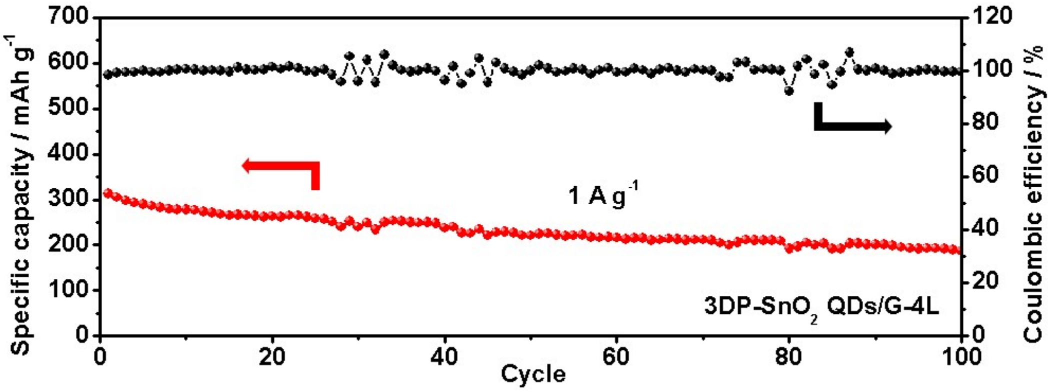

Fig. S12. Cycle performances of 3DP-SnO_2 QDs/G architectures at a current density of 1A g^{-1}. A stable specific capacity of 187.4 mAh g^{-1} can be retained after 100 cycles.

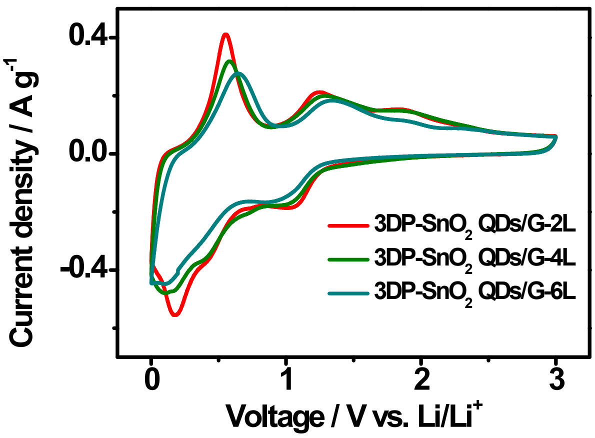

Fig. S13. Comparison of CV curves of 3DP-SnO_2 QDs/G architectures with different printed layers.

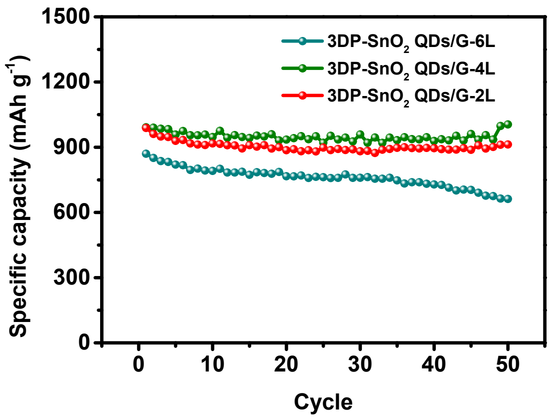

Fig. S14. The specific capacities of 2-layer, 4-layer and 6-layer 3DP-SnO_2 QDs/G architectures. The 3DP-SnO_2 QDs/G with 6 layers shows slightly lower spcific capacities than the samples with 2 layers and 4 layers.

Table S1. Kinetics parameters of 3DP-SnO_2 QDs/G, SnO_2 QDs/G and SnO_2 QDs architectures.

	3DP-SnO_2 QDs/G	SnO_2 QDs/G	SnO_2 QDs
R_1 [Ω]	6.8	6.5	3.9
R_2 [Ω]	19.9	11.0	8.3
R_3 [Ω]	5.4	28.1	54.8